IEEE Access
Multidisciplinary | Rapid Review | Open Access Journal

Received September 18, 2020, accepted October 2, 2020, date of publication October 8, 2020, date of current version October 21, 2020.

Digital Object Identifier 10.1109/ACCESS.2020.3029567

A Time-Robust Digital Self-Interference Cancellation in Full-Duplex Radios: Receiver Design and Performance Analysis

YIMIN HE, (Member, IEEE), HONGZHI ZHAO, (Graduate Student Member, IEEE), WENBO GUO, (Member, IEEE), SHIHAI SHAO, (Member, IEEE), AND YOUXI TANG, (Member, IEEE)

National Key Laboratory of Science and Technology on Communications, University of Electronic Science and Technology of China, Chengdu 611731, China

Corresponding authors: Hongzhi Zhao (lyn@uestc.edu.cn) and Shihai Shao (sh@uestc.edu.cn)

This work was supported in part by the National Key Research and Development Program of China under Grant 254, in part by the National Natural Science Foundation of China under Grant 61771107, Grant 61701075, Grant 61601064, and Grant 61531009; and in part by the Sichuan Science and Technology Program under Grant 2019JDRC0006.

ABSTRACT In full-duplex radios, precise time synchronization between the received and reconstructed self-interference (SI) is the basis of the effective SI cancellation (SIC). However, due to the impacts of the hardware imperfections and the propagation environment, perfect time synchronization is impossible. More seriously, the time-varying SI propagation channel aggravates the difficulty of time synchronization. To overcome the above problems, a time-robust digital SIC (TR-DSIC) is proposed in this article, as a novel scheme to address the time synchronization error (timing error). Firstly, by comprehensively considering nonlinear distortion and multipath propagation with different time delays and time-varying gains, a revised general memory polynomial (RGMP) model of the received SI is presented. Then, based on the RGMP model of the received SI, the TR-DSIC is proposed to cancel the SI in the digital domain, which is robust to arbitrary timing error and no need additional processing for it. Finally, the performance of the proposed TR-DSIC is analyzed under imperfect estimations of the polynomial coefficients. The analytical expression of the variance of the estimation error is presented here, and the closed-form expression of the residual SI power introduced by imperfect estimations of the polynomial coefficients is derived. Simulation results reveal that the TR-DSIC is capable of eliminating the influence of arbitrary timing error. Specially, when the maximum timing error is $0.5T_s$ for the SI multipath channel, the TR-DSIC outperforms the traditional DSIC without considering the timing error between the reconstructed and received SI by 5.2 dB.

INDEX TERMS Full-duplex, self-interference cancellation, timing error, nonlinear distortion, multipath.

I. INTRODUCTION

Full-duplex (FD) is capable of doubling the spectrum efficiency by transmitting and receiving signals simultaneously at the same carrier frequency, which has become a key technology in wireless communication [1]. However, such benefit is based on effective self-interference (SI) cancellation due to the leakage of the high-power signal sent by the transmitting antenna [2].

Generally, digital SI cancellation (SIC) exploits the fact that the FD receiver has knowledge of the intended transmit signal in the digital domain, making it possible to reconstruct the SI and then cancel it. However, due to the impacts of the hardware imperfections and the propagation environment, perfect time synchronization between the reconstructed and received SI is almost impossible [3]. The SI propagation channel usually includes the direct path (DP) through the antenna interface device, which has a limited isolation for the high-power transmitted signal, and the multipath reflection paths (RPs) that are created by objects within the environment [4]. Generally, the delay from each path consists of the integral part and the fractional part. More specifically, the integer part is an integral multiple of the sampling period, which is easy to be compensated for the reconstructed SI by time synchronization operation. Nevertheless, the fractional part that lower than the sampling accuracy will introduce the

The associate editor coordinating the review of this manuscript and approving it for publication was Tianhua Xu.

time synchronization error (timing error), which is hard to estimate for compensation and will lead to incomplete elimination of the multipath components [5]. Besides, in contrast to the fairly static DP coupling, the RP signals are dynamic because of the influence of the surroundings [6]. In other words, the SI multipath channel is time-varying and thus aggravates the difficulty of the time synchronization, which must be addressed accordingly. Moreover, with the increase of the transmitting power, the inherent nonlinearity of power amplifier (PA) will be introduced to the received SI unavoidably, further increasing the complexity of the estimation of the timing error [7].

In recent years, many existing works dealing with the above problems always suppose that just the integral part of the SI multipath delay exists [8]–[11]. For instance, the authors in [8] introduce a model for the coupling interference of FD systems, in which the integral time offset is considered, but the inter-symbol interference introduced by the fractional time offset is ignored. A novel transceiver antenna selection strategy for FD amplify-forward multi-input multi-output two-way relay networks is proposed in [9] without considering the decision-making error introduced by the fractional parts of the multipath delays. A novel adaptive SIC solution and the total integrated cancellation performance of a mobile single-antenna inband FD transceiver are investigated in [10], in which the fractional parts of the multipath delays are not considered under low processing rate. In [11], an FD transceiver with a two-stage analog interference cancellation architecture is proposed, where a nonlinear model is particularly designed in the stage-II cancellation to build a multipath canceling signal in the digital domain, assuming the multipath delays are integer multiple of the sampling periods. However, the fractional part of the SI multipath delay is inherent, which acts as the timing error and degrades the SIC performance [12].

In addition, by assuming the SI multipath delays are known at the receiver, some investigations are conducted to tackle the timing error [13], [14]. In [13], a digital postprocessing is applied to mitigate the imperfections of the analog to digital converter (ADC), where the time-mismatch errors are assumed to be known at the receiver. A variable fractional delay finite impulse response (FIR) filter is exploited in [14] to generate a fractional delay to synchronize the received SI and the reconstructed SI in the digital domain, in which the fractional delay should be estimated as the filter input. However, perfect estimation of the timing error is difficult and complex, leading to more resource consumption and additional processing for it.

Motivated by the above problem, in this article, a time-robust digital SIC (TR-DSIC) is proposed to simultaneously address nonlinear distortion and multipath propagation with arbitrary time delays (including both integral parts and fractional parts) and time-varying gains. Besides, considering a practical scenario that the estimation of the polynomial coefficient based on the least squares (LS) algorithm is performed under the existence of the desired signal, which introduces the estimation error of the polynomial coefficient. Therefore, the SIC performance of the proposed TR-DSIC is analyzed with the estimation error, providing guidance and theoretical support to design practical FD receivers with TR-DSIC. The main contributions are summarized as follows.

- Firstly, a TR-DSIC is proposed to simultaneously tackle the nonlinear distortion and multipath propagation with arbitrary time delays (including both integral parts and fractional parts), which is robust to arbitrary timing error between the reconstructed SI and the received SI, and no need additional processing for it. A revised general memory polynomial (RGMP) model of the received SI is presented with the above issue. Based on the RGMP model of the received SI, the TR-DSIC with optimal estimation of the polynomial coefficient under the LS criterion is given.
- Secondly, two issues of the proposed TR-DSIC in engineering implementation are discussed. On the one hand, as a measure of complexity, the minimum number of taps to achieve a certain SIC capability in the SI reconstruction operation is analyzed, providing guidance for future engineering. On the other hand, to track the time-varying SI channel, an iterative algorithm for the estimation of the polynomial coefficient is applied.
- Finally, the SIC performance of the proposed TR-DSIC is analyzed under imperfect LS-based estimations of the polynomial coefficients. The analytical expression of the variance of the estimation error is presented, and the closed-form expression of the residual SI power introduced by imperfect estimations of the polynomial coefficients is derived.

The rest of this article is organized as follows. Section II provides the RGMP model of the received SI with the nonlinear distortion and time-varying SI multipath channel, where the multipath delay includes both integer part and fractional part. Section III proposes the TR-DSIC with optimal estimation of the coefficient under the LS criterion. Section IV analyzes the complexity of the proposed TR-DSIC, and its adaptive implementation architecture is proposed. The SIC performance of the proposed TR-DSIC under imperfect estimations of the polynomial coefficients is analyzed in Section V. Simulation results are presented in Section VI to verify our analyses. Finally, Section VII concludes this article.

II. SELF-INTERFERENCE MODEL

Fig. 1 depicts a FD transceiver with the proposed TR-DSIC. Assuming the original SI data $x(n)$ suffers from the nonlinear distortion at the transmitting link and converts to $x_{NL}(n)$. After passing through the SI propagation channel, which introduces different time delays and time-varying gains, the SI is received as $y(n)$, whose polynomial model is derived in this section.

A. EFFECT OF NONLINEAR DISTORTION

With the increase of the transmitting power, nonlinear distortion is always introduced by imperfect devices in the FD

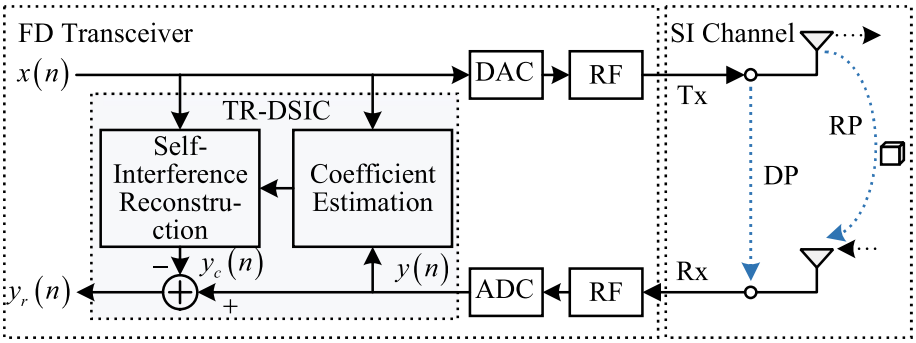

FIGURE 1. Diagram of a FD transceiver, in which the proposed TR-DSIC is implemented to cancel the SI in the digital domain.

link. A memory polynomial (MP) model is used to describe the nonlinearity [15], thus the SI with nonlinear distortion can be written as

$$x_{NL}(n) = \sum_{k=0}^{K-1}\sum_{q=0}^{Q-1} a_{kq} x(n-q)\,|x(n-q)|^{2k}, \tag{1}$$

where $2k-1$ and Q denote the highest nonlinearity order and memory order, respectively. a_{kq} and $x_{kq}(n) = x(n-q)\,|x(n-q)|^{2k}$ are used to characterize the nonlinearity, which respectively denote the MP kernel and the nonlinear component. Besides, compared with the SI channel, the MP kernel changes slowly and can be regarded as a constant.

B. EFFECT OF MULTIPATH

As shown in Fig. 1, due to the existence of the RPs, the effect of the multipath should be considered in the modeling of the received SI. Assuming the delay of the i-th path is τ_i for the reconstructed SI, which is an integral multiple of the sampling period. However, the actual delay of the i-th path is $\tau_i + \Delta\tau_i$ for the received SI, where $\Delta\tau_i$ is the timing error. Therefore, the digital version of the received SI is given by

$$y(n) = \sum_{i=1}^{L} h_i(n) x_{NL}(n - D_i - \Delta D_i) + z(n), \tag{2}$$

where $z(n)$ is the noise at the receiver. $h_i(n)$ is the time-varying channel gain of the i-th path after analog SIC. $D_i = \tau_i/T_s$ is the normalized delay, and $\Delta D_i = \Delta\tau_i/T_s$ is the normalized timing error, where T_s is the sampling interval of the ADC.

ΔD_i generally consists of the integer part $\Delta D_{I,i}$ and the fractional part $\Delta D_{F,i}$, i.e. $\Delta D_i = \Delta D_{I,i} + \Delta D_{F,i}$. $\Delta D_{I,i}$ is an integral multiple of the sampling period, which is easy to be compensated for the reconstructed SI by time synchronization operation, thus the integer timing error $\Delta D_{I,i}$ can be regard as 0. However, $\Delta D_{F,i}$ is fractional multiple of the sampling period, which is often omitted in the existing literature and reduces the accuracy of the SI modeling. Therefore, this article focuses on the fractional timing error.

Substituting (1) into (2), $y(n)$ can be written as

$$\begin{aligned} y(n) &= \sum_{i=1}^{L} h_i(n) \sum_{k=0}^{K-1}\sum_{q=0}^{Q-1} a_{kq} x_{kq}\left(n - D_i - \Delta D_{F,i}\right) + z(n) \\ &= \sum_{i=1}^{L} h_i(n) \sum_{k=0}^{K-1}\sum_{q=D_i}^{Q+D_i-1} a_{kq} x_{kq}\left(n - \Delta D_{F,i}\right) + z(n). \end{aligned} \tag{3}$$

C. EFFECT OF FRACTIONAL TIMING ERROR

Considering $x_{kq}\left(n - \Delta D_{F,i}\right)$ is the copy of $x_{kq}(n)$ with the fractional timing error $\Delta D_{F,i}$, thus it can be expressed as follows by utilizing the ideal fractional delay model [16]

$$\begin{aligned} x_{kq}\left(n - \Delta D_{F,i}\right) &= x_{kq}(n) \otimes h_{\Delta D_{F,i}}(n) \\ &= \sum_{j=-\infty}^{+\infty} x_{kq}(n-j)\, h_{\Delta D_{F,i}}(j), \end{aligned} \tag{4}$$

where $\otimes$ denotes the convolution operation, and the coefficient of the ideal fractional delay model can be defined as

$$h_{\Delta D_{F,i}}(n) = \mathrm{sinc}\left(n - \Delta D_{F,i}\right) = \frac{\sin\left[\left(n - \Delta D_{F,i}\right)\pi\right]}{\left(n - \Delta D_{F,i}\right)\pi}. \tag{5}$$

Besides, note that $x_{kq}(n-j) = x_{k,q+j}(n)$.

In practice, infinite impulse response (IIR) filter is impossible to implement, so we truncate the coefficients of the fractional delay model from $-M$ to M, thus (4) can be written as

$$x'_{kq}\left(n - \Delta D_{F,i}\right) = \sum_{j=-M}^{M} h_{\Delta D_{F,i}}(j)\, x_{kq}(n-j). \tag{6}$$

Defining the normalized mean square error (NMSE) as (7), thus the impact of M on the accuracy of the fractional delay model for different ΔD_F is shown in Fig. 2. It can be seen that the NMSE is less than $10^{-2.7}$ when $M = 5$.

$$NMSE = \frac{\mathrm{E}\left\{\left|x'_{kq}\left(n - \Delta D_{F,i}\right) - x_{kq}\left(n - \Delta D_{F,i}\right)\right|^2\right\}}{\mathrm{E}\left\{\left|x_{kq}\left(n - \Delta D_{F,i}\right)\right|^2\right\}}. \tag{7}$$

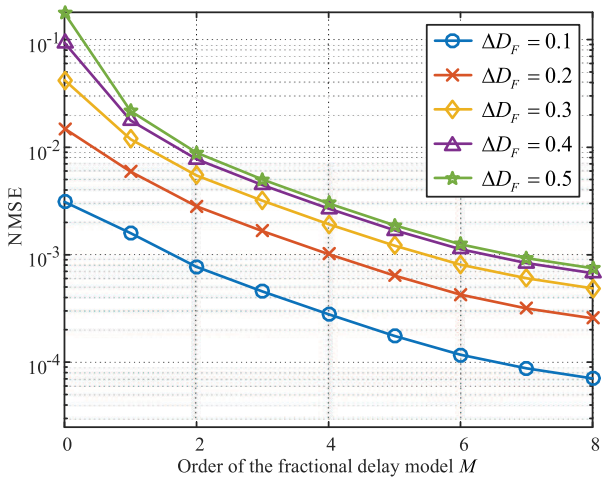

FIGURE 2. The impact of M on the accuracy of the fractional delay model for different fractional timing error ΔD_F.

D. POLYNOMIAL MODEL OF SELF-INTERFERENCE

After nonlinear distortion and multipath propagation, the received SI $y(n)$ consists of the linear SI, the nonlinear SI, and the receiver noise. For convenience, we omit $z(n)$ in the following derivation. Combining (1), (3), and (6), the received SI can be expressed in polynomial term as

$$\begin{aligned} y(n) &= \sum_{i=1}^{L}\sum_{k=0}^{K-1}\sum_{q=D_i}^{Q+D_i-1}\sum_{j=-M}^{M}\alpha_{ikqj}(n)x_{kq}(n-j) \\ &= \sum_{i=1}^{L}\sum_{k=0}^{K-1}\sum_{q=D_i}^{Q+D_i-1}\sum_{m=-M+q}^{M+q}\alpha_{ikqm}(n)x_{km}(n), \end{aligned} \tag{8}$$

where $\alpha_{ikqj}(n) = h_i(n)a_{kq}h_{\Delta D_{F,i}}(j)$ and $\alpha_{ikqm}(n) = h_i(n)a_{kq}h_{\Delta D_{F,i}}(m-q)$ are the time-varying coefficients related with the variables i, k, q, j, and m, where $m = q + j$.

III. TIME-ROBUST DIGITAL SELF-INTERFERENCE CANCELLATION

A. REVISED GENERAL MEMORY POLYNOMIAL MODEL OF SELF-INTERFERENCE

The polynomial expression of the SI has been explained in (8), where $x_{km}(n)$ is the nonlinear component, and $\alpha_{ikqm}(n)$ is the comprehensive coefficient for $x_{km}(n)$ which associated with i, k, q, and m. To simplify (8), the following transformation is made

$$\begin{aligned} y(n) &= \sum_{i=1}^{L}\sum_{k=0}^{K-1}\sum_{m=-M+D_i}^{M+Q+D_i-1}\sum_{q=D_i}^{Q+D_i-1}\alpha'_{ikqm}(n)x_{km}(n) \\ &= \sum_{m=-M+D_{I,min}}^{M+Q+D_{I,\max}-1}\sum_{k=0}^{K-1}\sum_{i=1}^{L}\sum_{q=D_i}^{Q+D_i-1}\alpha''_{ikqm}(n)x_{km}(n) \\ &= \sum_{m=-M+D_{I,min}}^{M+Q+D_{I,\max}-1}\sum_{k=0}^{K-1}\omega_{km}(n)\,x_{km}(n), \end{aligned} \tag{9}$$

where D_i is an integer, thus $D_{I,\max} = \max(D_i)$ and $D_{I,\min} = \min(D_i)$ denote the maximum and minimum integer multipath delay of the SI after passing through the multipath channel, respectively. $\omega_{km}(n)$ denotes the simplified polynomial coefficient, which is given by

$$\omega_{km}(n) = \sum_{i=1}^{L}\sum_{q=D_i}^{Q+D_i-1} h_i(n)a_{kq}h''_{\Delta D_{F,i}}(m-q), \tag{10}$$

where $\alpha'_{ikqm}(n)$ and $\alpha''_{ikqm}(n)$ are respectively given by

$$\alpha'_{ikqm}(n) = h_i(n)a_{kq}h'_{\Delta D_{F,i}}(m-q), \tag{11}$$

$$\alpha''_{ikqm}(n) = h_i(n)a_{kq}h''_{\Delta D_{F,i}}(m-q), \tag{12}$$

where $h'_{\Delta D_{F,i}}(m-q)$ is the extension of $h_{\Delta D_{F,i}}(m-q)$, and $h''_{\Delta D_{F,i}}(m-q)$ is the extension of $h'_{\Delta D_{F,i}}(m-q)$. They are defined as

$$h'_{\Delta D_{F,i}}(m-q) = \begin{cases} h_{\Delta D_{F,i}}(m-q), & -M \le m-q \le M \\ 0, & \text{others}, \end{cases} \tag{13}$$

$$h''_{\Delta D_{F,i}}(m-q) = \begin{cases} h'_{\Delta D_{F,i}}(m-q), & -M+D_i \le m \le -M+Q+D_i-1 \\ 0, & \text{others}. \end{cases} \tag{14}$$

Through the above transformation, the polynomial coefficient is finally simplified to be $\omega_{km}(n)$, which reduces the dimensions. (9) is called as the RGMP model of the SI, it adds a revise of the fractional timing error based on the generalized MP model in [17], which improves the accuracy of the model used to describe the received SI.

B. LS-BASED SOLUTION

By assuming the SI multipath channel is block fading during the training period [18], the LS-based solution can be presented. Therefore, the RGMP model can be rewritten in a matrix form as

$$\mathbf{Y} = \mathbf{X}^T\Omega, \tag{15}$$

where

$$\mathbf{Y} = \begin{bmatrix} y(1) & y(2) & \cdots & y(N) \end{bmatrix}^T, \tag{16}$$

$$\mathbf{X} = \begin{bmatrix} \mathbf{X}_1 & \mathbf{X}_2 & \cdots & \mathbf{X}_N \end{bmatrix}^T, \tag{17}$$

$$\Omega = \begin{bmatrix} \omega_{1,-M+D_{I,\min}} & \cdots & \omega_{1,M+Q+D_{I,\max}-1} \\ \cdots & \omega_{k,m} & \cdots & \omega_{K,M+Q+D_{I,\max}-1} \end{bmatrix}^T. \tag{18}$$

The vectors $\mathbf{X}_n$, $n = 1, 2, \cdots, N$ in (17) are defined as

$$\mathbf{X}_n = \begin{bmatrix} \mathbf{X}_{n,0}^T & \mathbf{X}_{n,1}^T & \cdots & \mathbf{X}_{n,K\text{-}1}^T \end{bmatrix}^T, \tag{19}$$

where $\mathbf{X}_{n,k}$, $k = 1, 2, \cdots, K$ are defined as

$$\mathbf{X}_{n,k} = \begin{bmatrix} x_{k,0}(n) & x_{k,1}(n) & \cdots & x_{k,Q-1}(n) \end{bmatrix}^T. \tag{20}$$

The optimum coefficient estimation $\hat{\Omega}$ can be reformulated by operating LS algorithm in (15) as [19]

$$\hat{\Omega} = \left(\mathbf{X}^H\mathbf{X}\right)^{-1}\mathbf{X}^H\mathbf{Y}, \tag{21}$$

where $\mathbf{X}^H$ denotes the complex conjugate transpose of $\mathbf{X}$.

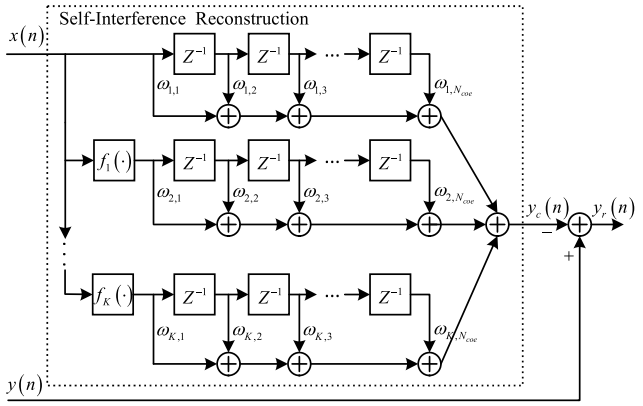

FIGURE 3. The implementation architecture of the SI reconstruction module in the proposed TR-DSIC.

Therefore, the reconstructed SI $y_c(n)$ can be expressed as

$$y_c(n) = \mathbf{X}_n^T \hat{\Omega}, \tag{22}$$

and the residual SI is given by

$$y_r(n) = y(n) - y_c(n) = \mathbf{X}_n^T \left(\Omega - \hat{\Omega}\right). \tag{23}$$

IV. IMPLEMENTATION ARCHITECTURE AND ANALYSIS

As show in Fig. 3, the SI reconstruction module in the proposed TR-DSIC consists of the nonlinear mapping functions and the linear filter bank. The linear filter bank is implemented by configuring K adaptive filters in parallel. Besides, $f_k(\cdot), k = 1, 2, \cdots, K$ denote the nonlinear mapping functions, defined as $f_k(x) = x|x|^{2k}$. In engineering implementation, the complexity of the proposed TR-DSIC and its ability to cope with environmental changes are two important issues of concern, which will be analyzed below.

On the one hand, the complexity of the proposed TR-DSIC is measured by the number of taps. According to (9), the minimum number of the taps can be derived as

$$N_{\min} = \min\left(N_{tap}\right) = K\left[2M + Q + \Delta D_I\right], \tag{24}$$

where N_{tap} denotes the actual taps number. $\Delta D_I = D_{I,\max} - D_{I,\min}$ denotes the integer delay spread. As we can see, the minimum number of the taps depends on the nonlinearity order K, the memory order of the nonlinearity Q, the order of the fractional delay model M, and the integer delay spread ΔD_I. However, N_{min} is independent of the multipath number L. Especially, for given K, Q, M, and ΔD_I, keep increasing the taps more than N_{min} is invalid to improve SIC performance, which is verified by following simulations.

On the other hand, to track the time-varying channel, the recursive LS (RLS) algorithm is applied to estimate the time-varing coefficients $\omega_{km}(n), k = 1, 2, \cdots, K, m = 1, 2, \cdots, N_{coe}$, due to its excellent real-time performance and convergence behavior. The RLS-based coefficient estimation applied in the TR-DSIC is shown in Algorithm 1 [20]. By adjusting the forgetting factor λ, the output of the RLS algorithm can follow the change of the environment, thus the estimations of the polynomial coefficients are able to track the time-varying SI channel.

Algorithm 1 RLS Algorithm

1: Initialization: setting $\mathbf{P}(0) = \delta^{-1}\mathbf{I}$, $\hat{\Omega}(0) = \mathbf{0}$ (δ: a very small positive number).
2: For every index n, repeat

$$\mathbf{k}(n) = \frac{\mathbf{P}(n-1)\mathbf{X}(n)}{\lambda + \mathbf{X}^{\mathrm{H}}(n)\mathbf{P}(n-1)\mathbf{X}(n)} \tag{25}$$

$$\xi(n) = y(n) - \hat{\Omega}^H(n-1)\mathbf{X}(n), \tag{26}$$

$$\hat{\Omega}(n) = \hat{\Omega}(n-1) + \mathbf{k}(n)\xi^*(n), \tag{27}$$

$$\mathbf{P}(n) = \lambda^{-1}\mathbf{P}(n-1) - \lambda^{-1}\mathbf{k}(n)\mathbf{X}^{\mathrm{H}}(n)\mathbf{P}(n-1), \tag{28}$$

V. PERFORMANCE ANALYSIS OF TR-DSIC WITH ESTIMATION ERROR

A. LS-BASED ESTIMATION ERROR

Based on the proposed TR-DSIC, the FD receiver is able to cancel the SI under the imperfect situation mentioned above, in which the polynomial coefficients are estimated offline, i.e. without the desired signal. Considering a practical FD communication, where the SI and the desired signal are both received by the receiver, thus the estimation errors of the polynomial coefficients will be introduced by the desired signal. The received signal is given by

$$y(n) = d_1(n) + d_2(n), \tag{29}$$

where $d_1(n)$ denotes the SI, and $d_2(n)$ denotes the combined signal of desired signal and noise. Therefore, the LS-based coefficient estimation $\hat{\Omega}$ can be written as

$$\hat{\Omega} = \left(\mathbf{X}^H\mathbf{X}\right)^{-1}\mathbf{X}^H\mathbf{d}_1 + \left(\mathbf{X}^H\mathbf{X}\right)^{-1}\mathbf{X}^H\mathbf{d}_2, \tag{30}$$

where $\mathbf{X}$ is defined in (17). Besides, $\mathbf{d}_1$ and $\mathbf{d}_2$ has a similar structure to $\mathbf{y}$.

Neglecting the noise, the contribution to the coefficient estimations due to the desired signal $d_2(n)$ is given by the second term in (30). Defining the error term as $\hat{\Omega}_2$. It can be represented as

$$\hat{\Omega}_2 = \left(\mathbf{X}^H\mathbf{X}\right)^{-1}\mathbf{X}^H\mathbf{d}_2. \tag{31}$$

Assuming $d_2(n)$ is zero-mean and uncorrelated with $d_1(n)$, thus the autocorrelation matrix of $\hat{\Omega}_2$ can be written as

$$\begin{aligned}\mathbf{R} &= \mathrm{E}\left\{\hat{\Omega}_2\hat{\Omega}_2^H\right\} \\ &= P\{d_2(n)\}\left(X^H X\right)^{-1},\end{aligned} \tag{32}$$

where $P\{\cdot\}$ denotes the power of the signal. Assuming the taps number used in the TR-DSIC is $K \times Q'$, where $Q' = 2M + Q + \Delta D_I$ denotes the total extension of the memory order. Therefore, $\hat{\Omega}_2$ is of dimension $KQ' \times 1$, and $\mathbf{R}$ is of dimension $KQ' \times KQ'$.

(32) represents the covariance matrix of the estimation error for a particular reference signal $x(n)$. To find the covariance matrix of the estimation error for any reference signal, the expectation operation is performed on the above equation over the reference signal, thus the expectation of $\mathbf{R}$ can be written as

$$\mathrm{E}\{\mathbf{R}\} = P\{d_2(n)\}\,\mathrm{E}\left\{\left(X^H X\right)^{-1}\right\}. \tag{33}$$

According to (17), $X^H X$ can be written as

$$\mathbf{X}^H\mathbf{X} = \sum_{n=1}^{N}\mathbf{X}_n\mathbf{X}_n^H, \tag{34}$$

where $\mathbf{X}_n\mathbf{X}_n^H$ can be divided into $K \times K$ block matrices, each block can be expressed as $\mathbf{X}_{n,k_1}\mathbf{X}_{n,k_2}^H$, $k_1, k_2 = 0, 1, \ldots, K-1$ with dimension $Q' \times Q'$.

Due to the independence between the original SI data, it can be derived that

$$\mathrm{E}\left\{x_{k_1,m_1}(n)\,x_{k_1,m_1}(n)\right\} = \begin{cases} 0, & m_1 \neq m_2 \\ P^x_{k_1+k_2+1}, & m_1 = m_2, \end{cases} \tag{35}$$

where $P^x_{k_1+k_2+1}$ is defined as

$$P^x_{k_1+k_2+1} = \mathrm{E}\left\{|x(n)|^{2(k_1+k_2+1)}\right\}. \tag{36}$$

The above formula is called as the $2(k_1+k_2+1)$-th origin moment of the random variable $x(n)$, it can be calculated from the distribution of $x(n)$. For instance, according to the central limit theorem, when $x(n)$ is an orthogonal frequency division multiplexing (OFDM) modulated signal and the number of the subcarriers is large enough, $|x(n)|$ follows the Rayleigh distribution, thus the $2n$-th origin moment of $x(n)$ is given as $E\left\{|x(n)|^{2n}\right\} = 2^n n!\sigma^{2n}$.

Based on (36), the expected value of $\mathbf{X}_{n,k_1}\mathbf{X}_{n,k_2}^H$ is given by

$$\mathrm{E}\left\{\mathbf{X}_{n,k_1}\mathbf{X}_{n,k_2}^H\right\} = P^x_{k_1+k_2+1}\mathbf{I}. \tag{37}$$

Considering the term $\Im_n$, which represents the difference between the expected value and the observed value of $\mathbf{X}_n\mathbf{X}_n^H$. It can be written as

$$\Im_n = \mathbf{X}_n\mathbf{X}_n^H - \mathbf{R}_x, \tag{38}$$

where $\mathbf{R}_x = \mathrm{E}\left\{\mathbf{X}_n\mathbf{X}_n^H\right\}$ consists of the block matrix defined in (37). Substituting (38) into (34), $\mathbf{X}^H\mathbf{X}$ can be written as

$$\mathbf{X}^H\mathbf{X} = N\mathbf{R}_x + \sum_{n=1}^{N}\Im_n. \tag{39}$$

Defining a new variable $\mathbf{K}$ to denote $\left(\mathbf{X}^H\mathbf{X}\right)^{-1}$, thus it can be formulated that

$$\mathbf{R}_x\mathbf{K} = \left(\mathbf{X}^H\mathbf{X}\mathbf{R}_x^{-1}\right)^{-1} = \frac{1}{N}\left(\mathbf{I} + \frac{1}{N}\sum_{n=1}^{N}\Im_n\mathbf{R}_x^{-1}\right)^{-1}. \tag{40}$$

To obtain the estimation of the inverse sample covariance matrix, the above equation can be expanded by busing a second order Taylor series as

$$\mathbf{R}_x\mathbf{K} \approx \frac{1}{N}\left(\mathbf{I} - \frac{1}{N}\sum_{n=1}^{N}\Im_n\mathbf{R}_x^{-1} + \frac{1}{N^2}\sum_{n=1}^{N}\sum_{m=1}^{N}\Im_n\mathbf{R}_x^{-1}\Im_m\mathbf{R}_x^{-1}\right). \tag{41}$$

Noting $\mathbf{R}_x$ is a Hermite matrix, whose inverse exists, thus the expectation of the above equation can be given as

$$\mathrm{E}\{\mathbf{K}\} = \frac{1}{N}\mathbf{R}_x^{-1}\left(\mathbf{I} + \frac{1}{N^2}\sum_{n=1}^{N}\sum_{m=1}^{N}\mathrm{E}\left\{\Im_n\mathbf{R}_x^{-1}\Im_m\mathbf{R}_x^{-1}\right\}\right). \tag{42}$$

Matrix $\mathbf{K}$ can be divided into $K \times K$ block matrices. Substituting (56) into (42), the expectation of the $(i,j)^{th}$ sub-block of matrix $\mathbf{K}$ can be given as

$$\mathrm{E}\{\mathbf{K}_{i,j}\} = \frac{Q'}{N^2}\left[\sum_{c=0}^{K-1}\sum_{p=0}^{K-1}\sum_{l_1=0}^{K-1}\sum_{l_2=0}^{K-1}P^x_{c+l_1+p+l_2+2}r_{i,c}r_{l_1,p}r_{l_2,j} + \left(Nr_{i,j} - \sum_{c=0}^{K-1}r_{i,c}\right)\right]\mathbf{I}. \tag{43}$$

The total contribution of the estimation errors of the polynomial coefficients due to the desired signal can be calculated by finding the trace of the expectation of the autocorrelation matrix $\mathbf{R}$, which is given by

$$tr\left(\mathrm{E}\{\mathbf{R}\}\right) = \frac{Q'P\{d_2(n)\}}{N^2}\eta, \tag{44}$$

where η is a variable related to the power of the original SI data and the nonlinear order, which defined as

$$\eta = \sum_{c=0}^{K-1}\sum_{p=0}^{K-1}\sum_{l_1=0}^{K-1}\sum_{l_2=0}^{K-1}P^x_{c+l_1+p+l_2+2}r_{i,c}r_{l_1,p}r_{l_2,j} + \left(Nr_{i,j} - \sum_{c=0}^{K-1}r_{i,c}\right). \tag{45}$$

The variance of the LS-based estimation error is given in (44), which relates to the power of the desired signal, the sample length, the nonlinear order, the total extension of the memory order, and the power of the original SI data.

B. POWER OF RESIDUAL SELF-INTERFERENCE

The residual SI is defined in (23), considering the LS-based estimation errors of the polynomial coefficients introduced by the desired signal, the residual SI can be reformulated as

$$y_r(n) = \mathbf{X}_n^T\hat{\Omega}_2 = \sum_{k=0}^{K-1}\mathbf{X}_{n,k}^T\hat{\Omega}_{2,k}, \tag{46}$$

where $\hat{\Omega}_{2,k}$ is the estimation error of the polynomial coefficient corresponding to the k-th order nonlinear component with dimension $Q' \times 1$.

Therefore, the residual SI power under particular reference signal can be calculated as

$$\begin{aligned} &P\{y_r(n)\} \\ &= \mathrm{E}\left\{\left|\sum_{k=0}^{K-1}\mathbf{X}_{n,k}^{T}\hat{\Omega}_{2,k}\right|^2\right\} \\ &= \mathrm{E}\left\{\sum_{k_1=0}^{K-1}\sum_{k_2=0}^{K-1}\hat{\Omega}_{2,k_1}^{T}\mathbf{X}_{n,k_1}\mathbf{X}_{n,k_2}^{H}\hat{\Omega}_{2,k_2}^{*}\right\} \\ &= P_{2k+1}^{x}\hat{\Omega}_{2,k}^{H}\hat{\Omega}_{2,k}+\sum_{k_1=0}^{K-1}\sum_{k_2=0,k_2\neq k_1}^{K-1}P_{k_1+k_2+1}^{x}\hat{\Omega}_{2,k_1}^{H}\hat{\Omega}_{2,k_2}. \end{aligned} \tag{47}$$

Performing the expectation operation on the reference signal, (47) can be written as

$$\begin{aligned} &\mathrm{E}\{P[y_r(n)]\} \\ &\quad=\sum_{k=0}^{K-1}P_{2k+1}^{x}\mathrm{E}\left\{\hat{\Omega}_{2,k}^{H}\hat{\Omega}_{2,k}\right\} \\ &\qquad+\sum_{k_1=0}^{K-1}\sum_{k_2=0,k_2\neq k_1}^{K-1}P_{k_1+k_2+1}^{x}\mathrm{E}\left\{\hat{\Omega}_{2,k_1}^{H}\hat{\Omega}_{2,k_2}\right\}. \end{aligned} \tag{48}$$

Due to the independence between different coefficients, the second term in (48) can be calculated as 0. The result of the first term in (48) is given in (61), thus the expectation of the residual SI power can be written as

$$\mathrm{E}\{P[y_r(n)]\}=\frac{KQ'}{N}P\{d_2(n)\}, \tag{49}$$

It can be seen that the power of the residual SI relates to the nonlinear order, the total extension of the memory order, the power of the desired signal, and the sample length, but not to the SI power.

VI. SIMULATION RESULTS AND DISCUSSIONS

In this section, simulation results are provided to validate the proposed TR-DSIC. Firstly, the SIC performance of the TR-DSIC is simulated under imperfect estimations of the polynomial coefficients, demonstrating that the proposed TR-DSIC is able to suppress the SI to the noise floor under certain conditions. Next, the SIC ratio (SICR) curves of the TR-DSIC under different multipath conditions are given, showing the robustness of the proposed TR-DSIC to timing error. Finally, the performance comparison between the TR-DSIC and the traditional DSIC without considering the fractional timing error is carried out, revealing that the proposed TR-DSIC significantly enhances the DSIC performance.

A. SIMULATION SETUP

In the simulations, a 64 quadrature amplitude modulation (64QAM) modulated FD system is implemented with the bandwidth of 20 MHz in baseband. Assuming the power of the received SI after analog SIC is -30 dBm, and the noise floor is -90 dBm. The sampling frequency is 120 MHz, thus $T_s = 8.3$ ns. Besides, the SICR is calculated to evaluate the performance of the SIC, which is give by

$$\mathrm{SICR}=10\log_{10}\frac{P_0+P_N}{P_r+P_N}, \tag{50}$$

where P_0, P_N, and P_r denote the power of the SI, the noise, and the residual SI, respectively.

TABLE 1. Simulation condition for the TR-DSIC performance analysis.

K	Q	M	ΔD_I	L	delay vector $\mathbf{D}$	N_{tap}
3	3	3	1	2	[0.1, 1.3]	30

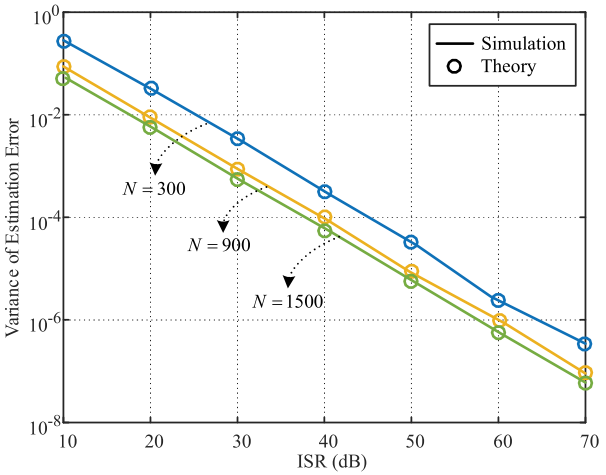

FIGURE 4. The variance of the estimation error vs. the ISR under the different cases of the sample number *N*.

B. SIMULATION RESULTS

To validate the correctness of the performance analysis based on the proposed TR-DSIC, under the simulation condition shown in the TABLE 1, Fig. 4 represents the effect of the interference to signal ratio (ISR) on the variance of the estimation error of the polynomial coefficient by adopting 100 Monte-Carlo simulations for each curve, which characterizes the accuracy of the LS estimation. For the convenience of the numerical calculation, the SI power is normalized to 0 dBm, and the power of the desired signal is adjustable to change the ISR. It can be seen that the simulation results agree well with the theoretical analysis presented in (44). With the increase of the ISR, the variance of the LS-based estimation error decreases. Besides, under the same value of the ISR, the longer the sample length, the smaller the variance of the LS-based estimation error, and the higher the estimation accuracy.

By adopting 100 Monte-Carlo simulations for each case of the sample number N, the effect of ISR on the power of the residual SI is depicted in Fig. 5 under the simulation condition shown in the TABLE 1. As we can see, the simulation results are coincident with the theoretical analysis given in (49). Besides, the power of the residual SI decreases

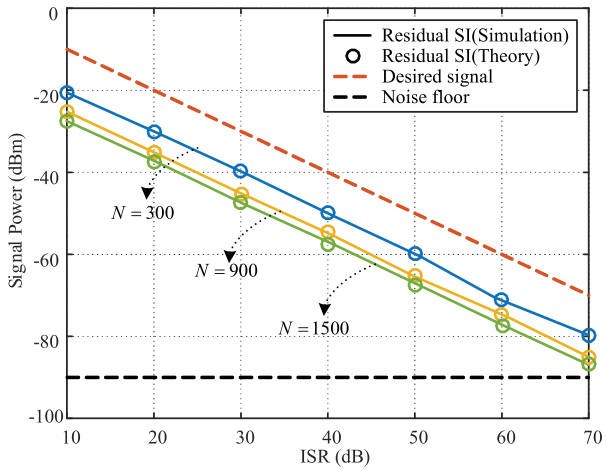

FIGURE 5. The power of the residual SI vs. the ISR under the different cases of the sample number N. Besides, the power of the desired signal and the noise floor is included to be a comparison.

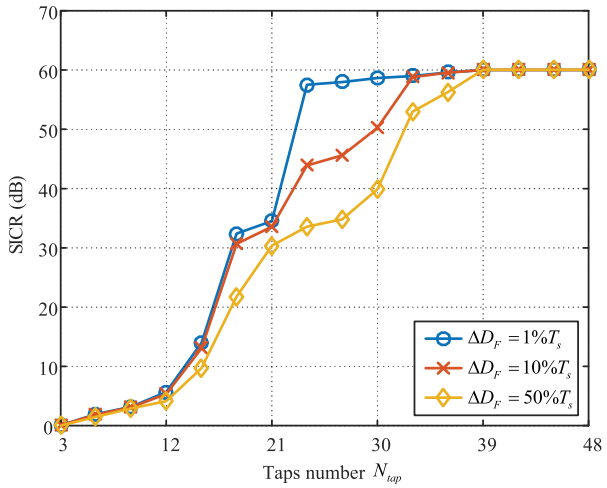

FIGURE 6. The SICR vs. the taps number under the different cases of the fractional timing error ΔD_F, where the corresponding $N_{min} = 39$.

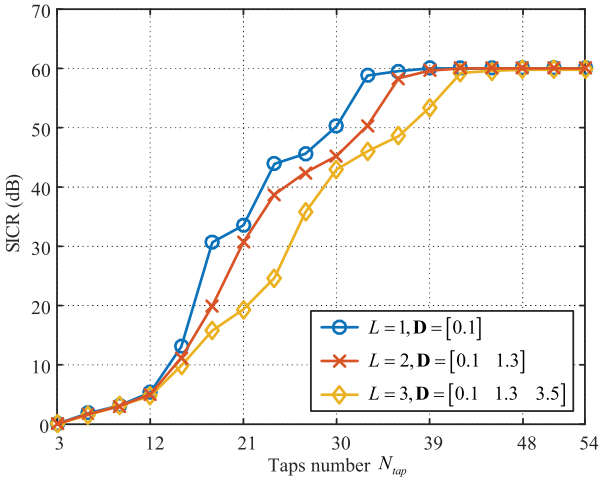

FIGURE 7. The SICR vs. the taps number under the different cases of the multipath, where the corresponding $N_{min} = 39, 42, 48$, respectively.

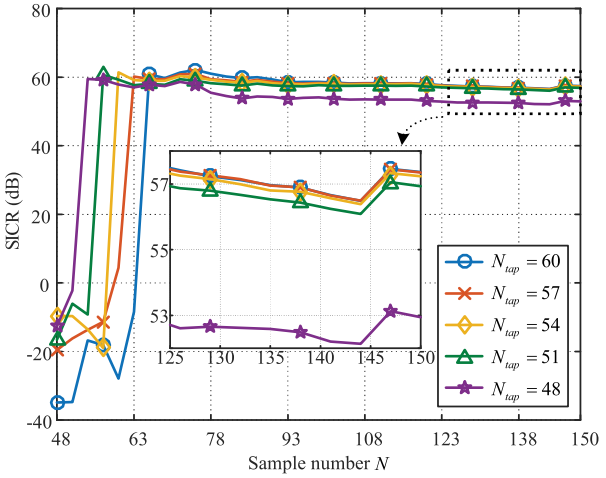

FIGURE 8. The SICR vs. the sample number under the different cases of the taps number N_{tap}. Besides, $N_{min} = 57$ under the given condition.

with the increase of the ISR, and the longer the sample length, the smaller the power of the residual SI, which reveals that the SIC performance can be improved by increasing the sample length. Specially, when $N = 1500$ and ISR$= 70$ dB, the residual SI is close to the noise floor, and the post signal to interference noise ratio can reach 17 dB.

To show the robustness of the proposed TR-DSIC to the fractional timing error, Fig. 6 depicts the effect of N_{tap} on the SICR with different ΔD_F, wherein $K = 3$, $Q = 3$, $L = 1$, $\Delta D_I = 0$, and $M = 5$, thus according to (24), N_{min} should be 39. One can see that the SICR increases with the increase of N_{tap}, and finally achieves 60 dB at the point of $N_{tap} = 39$, which agrees with the theoretical analysis. Besides, when $N_{tap} < 39$, the smaller the fractional timing error, the larger the SICR for fixed N_{tap}, indicating that the SIC performance of the proposed TR-DSIC is sensitive to ΔD_F when $N_{tap} < N_{min}$.

To show the effect of multipath on the performance of the proposed TR-DSIC, the SICR with respect to N_{tap} under different cases of the multipath is shown in Fig. 7, where $K = 3$, $Q = 3$, $M = 6$. The multipath number L varys from 1 to 3, and the multipath channel follows the Rice model [21], whose time delay vector $\mathbf{D}$ in each case is given in the legend of Fig. 7. As we can see, the integer delay spread $\Delta D_I = D_{I,\max} - D_{I,\min}$ are respectively 0, 1, 3, and the SICR converges to 60 dB at the corresponding points of $N_{tap} = 39, 42, 48$, which coincides with (24). It implies that the SIC performance of the TR-DSIC relates to the integer delay spread, but it has nothing to do with the multipath number.

The SICR changing with the sample number N is shown in Fig. 8, where $K = 3, Q = 3, L = 1, M = 5$, and $\Delta D_I = 6$, thus $N_{min} = 57$. To further observe the SIC performance with different N_{tap}, we set $N_{tap} = 60, 57, 54, 51, 48$, respectively. As we can see, when N_{tap} is less than 57, SICR decreases with N_{tap}, where the taps number is reduced by deleting the last column of the linear filter bank in Fig. 3. However, when N_{tap} is 57 and 60, the corresponding SICR tends to coincide, indicating that there is no further SICR improvement when the taps number is larger than N_{min}.

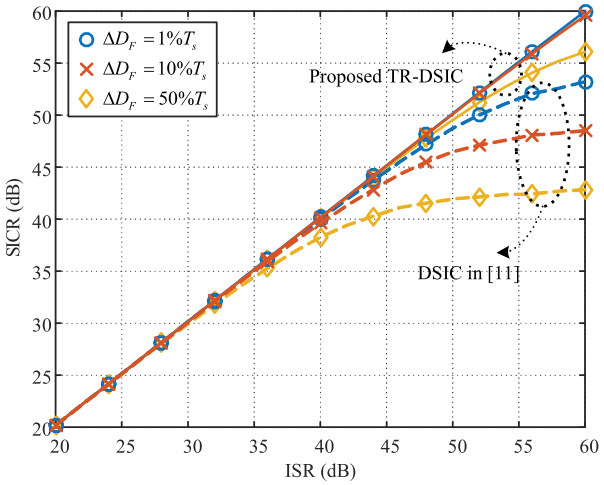

FIGURE 9. The SICR vs. the ISR under the different cases of the fractional timing error ΔD_F, utilizing the proposed TR-DSIC and the DSIC in [11], respectively.

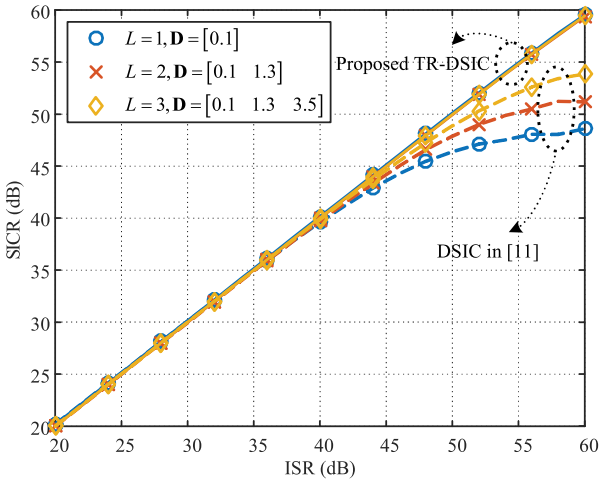

FIGURE 10. The SICR vs. the ISR under the different cases of the multipath, utilizing the proposed TR-DSIC and the DSIC in [11], respectively.

To compare the performance of the proposed TR-DSIC with the traditional DSIC without considering the fractional timing error, which is proposed in [11], Fig. 9 depicts the variance of the SICR with the ISR under different cases of the fractional timing error, in which the algorithms mentioned above are used to cancel the SI, respectively. The simulation conditions are the same as those in Fig. 6. It can be seen that when the ISR lager than 35 dB, the proposed TR-DSIC outperforms the DSIC in [11]. Besides, the larger the fractional timing error, the greater the performance gap between the two algorithms. Especially, when the fractional timing errors ΔD_F are $1\%T_s$, $10\%T_s$, and $50\%T_s$, compared with the DSIC in [11], the SICR of the proposed TR-DSIC is improved by 7 dB, 11 dB, and 12 dB, respectively.

Fig. 10 depicts the variance of the SICR with the ISR under different cases of the multipath, in which the TR-DSIC and the DSIC proposed in [11] are used to cancel the SI, respectively. The simulation conditions are the same as those in Fig. 7. As we can see, in the presence of the multipath, the proposed TR-DSIC enhances the SIC performance compared with the DSIC in [11], when ISR is greater than 40 dB. For example, in each case of the multipath corresponding to the legend in Fig. 10, where the maximum fractional timing error respectively are $10\%T_s$, $30\%T_s$, and $50\%T_s$, the proposed TR-DSIC outperforms the DSIC in [11] by 11 dB, 9 dB, 5.2 dB, respectively.

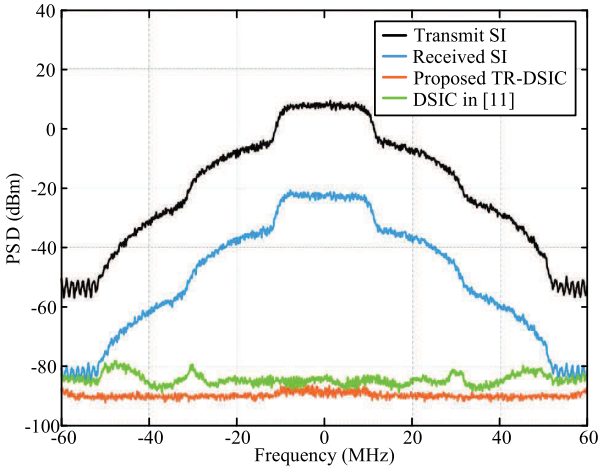

FIGURE 11. The PSD of the SI after utilizing the proposed TR-DSIC and the DSIC proposed in [11], respectively, where the multipath number is $L = 3$, and the corresponding time delay vector is [0.1, 1.3, 3.5].

Fig. 11 shows the corresponding power spectral density (PSD) of the SI after utilizing the proposed TR-DSIC and the DSIC proposed in [11], respectively. After passing through the transmitting link and multipath SI channel, where the multipath number is $L = 3$, and the corresponding time delay vector is [0.1, 1.3, 3.5], the spectrum of the received SI is distorted. Then, when the above two DSIC is carried out, the received SI is suppressed to -89.5 dBm and -84.3 dBm, respectively. Since the DSIC proposed in [11] is only capable of the SI multipath delay of integer sampling period, when the actual sampling rate of the ADC is relatively low and introduces fractional timing error, the algorithm in [11] can not accurately regenerate the SI signal, leading to 5.2 dB performance degradation compared with the proposed TR-DSIC. On the contrary, the proposed TR-DSIC can reconstruct the SI more accurately and cancel SI to the noise floor.

VII. CONCLUSION

In this article, a TR-DSIC is proposed to comprehensively tackle nonlinear distortion and multipath propagation with arbitrary time delays (including both integral parts and fractional parts) and time-varying gains in FD radios. First, an RGMP model of the received SI is presented by comprehensively considering the above issues. Next, the TR-DSIC is proposed to cancel the SI in the digital domain, which is robust to arbitrary timing error between the reconstructed SI and the received SI, and no need additional processing for it. Moreover, as a theoretical guide, the minimum number of the taps in the SI reconstruction operation is analyzed to

measure the complexity, and an RLS-based coefficient estimation algorithm is applied to track the time-varying SI channel. Finally, the SIC performance of the proposed TR-DSIC is analyzed under imperfect estimations of the polynomial coefficients, revealing that the residual SI power introduced by the estimation errors relates to the nonlinear parameters, the order of the fractional delay model, the maximum integer delay spread, the power of the desired signal, and the sample number for coefficient estimation, but not to the SI power. This article offers a novel idea for the development of digital SIC in FD, providing guidance and theoretical support to design practical FD receivers in the presence of the timing error.

APPENDIX A

To compute the expectation of the inverse sample covariance matrix, the expectation of matrix $\Im_n \mathbf{R}_x^{-1} \Im_m \mathbf{R}_x^{-1}$ is required. It can be formulated as

$$\Im_n \mathbf{R}_x^{-1} \Im_m \mathbf{R}_x^{-1} = \mathbf{X}_n \mathbf{X}_n^H \mathbf{R}_x^{-1} \mathbf{X}_m \mathbf{X}_m^H \mathbf{R}_x^{-1} - \mathbf{I}. \tag{51}$$

Similar to $\mathbf{R}_x$, dividing $\mathbf{R}_x^{-1}$ into $K \times K$ block matrices, where the $(i,j)^{th}$ sub-block is expressed as $\mathbf{r}_{i,j}$. Furthermore, the $(i,j)^{th}$ sub-block of $\mathbf{X}_n \mathbf{X}_n^H \mathbf{R}_x^{-1} \mathbf{X}_m \mathbf{X}_m^H \mathbf{R}_x^{-1}$ can be written as

$$\left\{ \mathbf{X}_n \mathbf{X}_n^H \mathbf{R}_x^{-1} \mathbf{X}_m \mathbf{X}_m^H \mathbf{R}_x^{-1} \right\}_{i,j} = \sum_{p=0}^{K\text{-}1} \sum_{l_1=0}^{K\text{-}1} \sum_{l_2=0}^{K\text{-}1} \mathbf{X}_{n,i} \mathbf{X}_{n,l_1}^H \mathbf{r}_{l_1,p} \mathbf{X}_{m,p} \mathbf{X}_{m,l_2}^H \mathbf{r}_{l_2,j}. \tag{52}$$

It can be found that each sub-block $\mathbf{r}_{i,j}$ is the product of a unit matrix and a constant, i.e. $\mathbf{r}_{i,j} = r_{i,j}\mathbf{I}$. Therefore, the element of the a-th row and b-th column of matrix $\mathbf{X}_{n,i} \mathbf{X}_{n,l_1}^H \mathbf{r}_{l_1,p} \mathbf{X}_{m,p} \mathbf{X}_{m,l_2}^H \mathbf{r}_{l_2,j}$ can be represented as

$$\left\{ \mathbf{X}_{n,i} \mathbf{X}_{n,l_1}^H \mathbf{r}_{l_1,p} \mathbf{X}_{m,p} \mathbf{X}_{m,l_2}^H \mathbf{r}_{l_2,j} \right\}_{a,b} = \sum_{c=0}^{Q'-1} x_{i,a}(n)\, x^*{}_{l_1,c}(n) x_{p,c}(m)\, x^*{}_{l_2,b}(m)\, r_{l_1,p} r_{l_2,j}. \tag{53}$$

Performing the expectation operation on the above equation and omitting the contributions of those terms of $a \neq b$ and $n \neq m$, then it can be derived that

$$\mathrm{E}\left\{ x_{i,a}(n)\, x^*{}_{l_1,c}(n) x_{p,c}(m)\, x^*{}_{l_2,b}(m) \right\} = \begin{cases} P^x_{i+l_1+p+l_2+2}, & c = a = b,\ n = m \\ 0, & \text{others.} \end{cases} \tag{54}$$

Combining (54), (53), and (52), the expectation of $\left\{ \mathbf{X}_n \mathbf{X}_n^H \mathbf{R}_x^{-1} \mathbf{X}_m \mathbf{X}_m^H \mathbf{R}_x^{-1} \right\}_{i,j}$ can be written as

$$\mathrm{E}\left\{ \mathbf{X}_n \mathbf{X}_n^H \mathbf{R}_x^{-1} \mathbf{X}_m \mathbf{X}_m^H \mathbf{R}_x^{-1} \right\}_{i,j} = \begin{cases} \left(\sum_{p=0}^{K\text{-}1} \sum_{l_1=0}^{K\text{-}1} \sum_{l_2=0}^{K\text{-}1} P^x_{i+l_1+p+l_2+2} r_{l_1,p} r_{l_2,j} \right) \mathbf{I}, & n = m \\ \mathbf{0}, & n \neq m. \end{cases} \tag{55}$$

Substituting (55) into (51), the expectation of the $(i,j)^{th}$ sub-block of matrix $\Im_n \mathbf{R}_x^{-1} \Im_m \mathbf{R}_x^{-1}$ can be given as

$$\mathrm{E}\left\{ \Im_n \mathbf{R}_x^{-1} \Im_m \mathbf{R}_x^{-1} \right\}_{i,j} = \begin{cases} \left(\sum_{p=0}^{K-1} \sum_{l_1=0}^{K-1} \sum_{l_2=0}^{K-1} P^x_{i+l_1+p+l_2+2} r_{l_1,p} r_{l_2,j} - 1 \right) \mathbf{I}, & n = m \\ \mathbf{0}, & n \neq m. \end{cases} \tag{56}$$

APPENDIX B

To calculate the autocorrelation matrix of the k-th error matrix $\hat{\Omega}_{2,k}$, similar to (32), it can be derived that

$$\mathbf{R}_k = \mathrm{E}\left\{ \hat{\Omega}_{2,k} \hat{\Omega}_{2,k}^H \right\} = P\{d_2(n)\} \left(\mathbf{X}_k^H \mathbf{X}_k \right)^{-1}, \tag{57}$$

where

$$\mathbf{X}_k = \begin{bmatrix} \mathbf{X}_{1,k} & \mathbf{X}_{2,k} & \cdots & \mathbf{X}_{N,k} \end{bmatrix}^T. \tag{58}$$

Performing the expectation operation on the above equation over the reference signal, the covariance matrix of error for any reference signal is given by

$$\mathrm{E}\{\mathbf{R}_k\} = P\{d_2(n)\}\, \mathrm{E}\left\{ \left(\mathbf{X}_k^H \mathbf{X}_k \right)^{-1} \right\}. \tag{59}$$

For different k, the expectation of matrix $\left(\mathbf{X}_k^H \mathbf{X}_k \right)^{-1}$ is given as [22]

$$\mathrm{E}\left\{ \left(\mathbf{X}_k^H \mathbf{X}_k \right)^{-1} \right\} = \frac{1}{N P^x_{2k+1}} \mathbf{I}. \tag{60}$$

The total contribution of the k-th estimated error of the TR-DSIC coefficients due to the desired signal can be calculated by finding the trace of the autocorrelation matrix $\mathbf{R}_k$, which is given by

$$\mathrm{E}\left\{ \hat{\Omega}_{2,k}^H \hat{\Omega}_{2,k} \right\} = tr(\mathbf{R}_k) = \frac{Q'}{N P^x_{2k+1}} P\{d_2(n)\}. \tag{61}$$

REFERENCES

[1] C. Baquero Barneto, T. Riihonen, M. Turunen, L. Anttila, M. Fleischer, K. Stadius, J. Ryynanen, and M. Valkama, "Full-duplex OFDM radar with LTE and 5G NR waveforms: Challenges, solutions, and measurements," *IEEE Trans. Microw. Theory Techn.*, vol. 67, no. 10, pp. 4042–4054, Oct. 2019.
[2] G. Liu, F. R. Yu, H. Ji, V. C. M. Leung, and X. Li, "In-band full-duplex relaying: A survey, research issues and challenges," *IEEE Commun. Surveys Tuts.*, vol. 17, no. 2, pp. 500–524, 2nd Quart., 2015.
[3] S. Shaboyan, E. Ahmed, A. S. Behbahani, W. Younis, and A. M. Eltawil, "Frequency and timing synchronization for in-band full-duplex OFDM system," in *Proc. IEEE Global Commun. Conf. (GLOBECOM)*, Singapore, Dec. 2017, pp. 1–7.
[4] K. E. Kolodziej, B. T. Perry, and J. S. Herd, "In-band full-duplex technology: Techniques and systems survey," *IEEE Trans. Microw. Theory Techn.*, vol. 67, no. 7, pp. 3025–3041, Jul. 2019.
[5] W. Guo, C. Li, H. Zhao, R. Wen, and Y. Tang, "Comprehensive effects of imperfect synchronization and channel estimation on known interference cancellation," *IEEE Trans. Veh. Technol.*, vol. 69, no. 1, pp. 457–470, Jan. 2020.

[6] H. Senol, X. Li, and C. Tepedelenlioglu, "Rapidly time-varying channel estimation for full-duplex Amplify-and-Forward one-way relay networks," *IEEE Trans. Signal Process.*, vol. 66, no. 11, pp. 3056–3069, Jun. 2018.
[7] D. Korpi, T. Riihonen, V. Syrjala, L. Anttila, M. Valkama, and R. Wichman, "Full-duplex transceiver system calculations: Analysis of ADC and linearity challenges," *IEEE Trans. Wireless Commun.*, vol. 13, no. 7, pp. 3821–3836, Jul. 2014.
[8] G. J. Gonzalez, F. H. Gregorio, J. Cousseau, T. Riihonen, and R. Wichman, "Generalized self-interference model for full-duplex multi-carrier transceivers," *IEEE Trans. Commun.*, vol. 67, no. 7, pp. 4995–5007, Jul. 2019.
[9] E. Fidan and O. Kucur, "Performance of transceiver antenna selection in two way full-duplex relay networks over Rayleigh fading channels," *IEEE Trans. Veh. Technol.*, vol. 67, no. 7, pp. 5909–5921, Jul. 2018.
[10] D. Korpi, Y.-S. Choi, T. Huusari, L. Anttila, S. Talwar, and M. Valkama, "Adaptive nonlinear digital self-interference cancellation for mobile inband full-duplex radio: Algorithms and RF measurements," in *Proc. IEEE Global Commun. Conf. (GLOBECOM)*, Dec. 2014, pp. 1–7.
[11] Y. Liu, P. Roblin, X. Quan, W. Pan, S. Shao, and Y. Tang, "A full-duplex transceiver with two-stage analog cancellations for multipath self-interference," *IEEE Trans. Microw. Theory Techn.*, vol. 65, no. 12, pp. 5263–5273, Dec. 2017.
[12] Y. Liu, X. Quan, W. Pan, S. Shao, and Y. Tang, "Performance analysis of direct-learning digital predistortion with loop delay mismatch in wideband transmitters," *IEEE Trans. Veh. Technol.*, vol. 65, no. 9, pp. 7078–7089, Sep. 2016.
[13] C. A. Schmidt, G. Gonzalez, F. Gregorio, J. E. Cousseau, T. Riihonen, and R. Wichman, "Compensation of ADC-induced distortion in broadband full-duplex transceivers," in *Proc. IEEE Int. Conf. Commun. Workshops (ICC Workshops)*, Paris, France, May 2017, pp. 1147–1152.
[14] C. Li, H. Zhao, F. Wu, and Y. Tang, "Digital self-interference cancellation with variable fractional delay FIR filter for full-duplex radios," *IEEE Commun. Lett.*, vol. 22, no. 5, pp. 1082–1085, May 2018.
[15] Z. Liu, X. Hu, T. Liu, R. Chen, X. Li, and W. Wang, "Predistortion with low feedback sampling rate for wideband nonlinear satellite downlinks," *IEEE Commun. Lett.*, vol. 23, no. 12, pp. 2367–2371, Dec. 2019.
[16] J. Selva, "An efficient structure for the design of variable fractional delay filters based on the windowing method," *IEEE Trans. Signal Process.*, vol. 56, no. 8, pp. 3770–3775, Aug. 2008.
[17] Y. Liu, X. Quan, W. Pan, S. Shao, and Y. Tang, "Nonlinear distortion suppression for active analog self-interference cancellers in full duplex wireless communication," in *Proc. IEEE Globecom Workshops (GC Wkshps)*, Austin, TX, USA, Dec. 2014, pp. 948–953.
[18] D. Liu, Y. Shen, S. Shao, Y. Tang, and Y. Gong, "On the analog self-interference cancellation for full-duplex communications with imperfect channel state information," *IEEE Access*, vol. 5, pp. 9277–9290, 2017.
[19] L. Guan and A. Zhu, "Optimized low-complexity implementation of least squares based model extraction for digital predistortion of RF power amplifiers," *IEEE Trans. Microw. Theory Techn.*, vol. 60, no. 3, pp. 594–603, Mar. 2012.
[20] E. M. Eksioglu and A. K. Tanc, "RLS algorithm with convex regularization," *IEEE Signal Process. Lett.*, vol. 18, no. 8, pp. 470–473, Aug. 2011.
[21] X. Wu, Y. Shen, and Y. Tang, "The power delay profile of the single-antenna full-duplex self-interference channel in indoor environments at 2.6 GHz," *IEEE Antennas Wireless Propag. Lett.*, vol. 13, pp. 1561–1564, 2014.
[22] D. Jovin Vasanth Kumar and R. Bhattacharjee, "Analysis of the LS estimation error for a MIMO system on a rician fading channel," in *Proc. IEEE Region 10 Conf. (TENCON)*, Nov. 2008, pp. 1–6.

YIMIN HE (Member, IEEE) was born in Yunnan, China, in 1996. She received the B.E. degree in communication engineering from the University of Electronic Science and Technology of China (UESTC), Chengdu, China, in 2018, where she is currently pursuing the Ph.D. degree in communication and information systems with the National Key Laboratory of Science and Technology on Communications. Her research interests include digital self-interference cancellation, physical layer security, full-duplex communications, and signal processing in wireless communications.

HONGZHI ZHAO (Graduate Student Member, IEEE) was born in Hebei, China, in 1978. He received the B.S., M.S., and Ph.D. degrees in communication engineering from the University of Electronic Science and Technology of China (UESTC), Chengdu, China, in 2001, 2004, and 2008, respectively. From 2006 to 2008, he was with the Positioning and Wireless Technology Center Laboratory (PWTC Lab), Nanyang Technology University, Singapore. He is currently with the National Key Laboratory of Science and Technology on Communications, UESTC, as a Professor. His research interests include antijamming technologies, full-duplex communications, and signal processing in wireless communications.

WENBO GUO (Member, IEEE) was born in Sichuan, China, in 1994. He received the B.E. degree in automation engineering from the University of Electronic Science and Technology of China (UESTC), Chengdu, China, in 2015, where he is currently pursuing the Ph.D. degree in communication and information systems with the National Key Laboratory of Science and Technology on Communications. His research interests include interference cancellation, physical layer security, full-duplex communications, and signal processing in wireless communications.

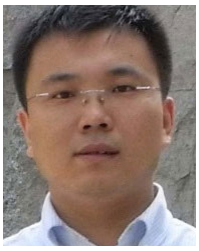

SHIHAI SHAO (Member, IEEE) was born in Liaoning, China, in 1980. He received the B.E. and Ph.D. degrees in communication and information systems from the University of Electronic Science and Technology of China, Chengdu, China, in 2003 and 2008, respectively.

Since 2008, he has been an Associate Professor with the National Key Laboratory of Science and Technology on Communications, University of Electronic Science and Technology of China. His research interests include wireless communications, spread spectrum, and multiple-input-multiple-output detection.

YOUXI TANG (Member, IEEE) was born in Henan, China, in 1964. He received the B.E. degree in radar engineering from the College of PLA Ordnance, Shijiazhuang, China, in 1985, and the M.S. and Ph.D. degrees in communication and information systems from the University of Electronic Science and Technology of China (UESTC), Chengdu, China, in 1993 and 1997, respectively. From 1998 to 2000, he was with Huawei Technologies Company Ltd., Shanghai, China, as a Program Manager, working in the area of IS-95 mobile communications and third-generation mobile communications. He is currently with the National Key Laboratory of Science and Technology on Communications, UESTC, as a Professor. His research interests include spread spectrum systems, wireless mobile systems with emphasis on signal processing in communications, and full-duplex communications.